Available online at www.sciencedirect.com
SCIENCE DIRECT®

Agricultural water management

Agricultural Water Management 73 (2005) 131–147

www.elsevier.com/locate/agwat

Subirrigation of land bordering small reservoirs in the semi-arid region in the Northeast of Brazil: monitoring and water balance

A.C.D. Antonino[a,*], C. Hammecker[b], S.M.L.G. Montenegro[c], A.M. Netto[a], R. Angulo-Jaramillo[d], C.A.B.O. Lira[a]

[a]*Departamento de Energia Nuclear, Universidade Federal de Pernambuco (UFPE), Av. Prof. Luiz Freire, 1000, Recife - PE, CEP 50740-540, Brazil*
[b]*Institut de Recherche pour le Développement, Dakar, Sénégal*
[c]*Departamento de Engenharia Civil, Universidade Federal de Pernambuco, Recife, Brazil*
[d]*Laboratoire d'étude des Transferts en Hydrologie et Environnement, LTHE, UMR 5564 CNRS, INPG, IRD, UJF, Grenoble, France*

Accepted 13 October 2004

Abstract

In Northeast Brazil, more than 70,000 small dams retain superficial runoff and underground water flow, creating small reservoirs. Recession agriculture consists of cropping the margins of the reservoirs, on slight slopes, while the water level progressively decreases, and it is a widespread cropping system in this area. The water balance for this particular system was quantified on two contiguous plots, one with "Marreca" grass (*Paspalum conjugatum* Berg.), a forage crop, and the other one on bare soil, in the recession zone of the basin of Flocos dam, municipality of Tuparetama, PE (7°36′S and 37°18′W). The soil, classified as Fluvent, consists of a superficial clay textured layer overlying a sandy layer. Next to the dam, a meteorological station was installed, equipped with automatic sensors for recording rainfall, air temperature and wind speed, and pan evaporation. In the reservoir, the water level was recorded. The plots were instrumented with one neutron probe access tube, one piezometer and tensiometers at different soil depths. Water retention and hydraulic conductivity characteristics were determined through field and laboratory measurements. The water balance was determined for the cropped and the bare soil plots, during 67 days. Average values for the actual evaporation and evapotranspiration rate, were respectively 5.0 and 8.0 mm day^{-1}, with an

* Corresponding author. Tel.: + 55 81 2126 8251; fax: +55 81 2126 8250.
E-mail address: acda@ufpe.br (A.C.D. Antonino).

doi:10.1016/j.agwat.2004.10.001

average reference evaporation rate of 8.7 mm day^{-1}. The contribution of the aquifer recharge to evaporative demand was estimated and found to be very important. Field observation and the estimated aquifer recharge from the reservoir suggest the presence of preferential flow. The study of water dynamics in this system is fundamental for establishing a basis for the sustainable development of agriculture in this area.

Keywords: Recession agriculture; Semi-arid; Water balance; Evapotranspiration

1. Introduction

In the semi-arid zone of the Brazilian Northeast region, river valleys, lowlands and the adjacent flat or slightly undulated areas, have the best potential for agricultural production, due to better water availability. Water collected in the catchment area, whether through intermittent rivers or underground flows, converges towards these areas, where traditionally small dams were built in order to retain water, and create small reservoirs. Soils are generally more than 1 m deep in these areas, and can store enough water to supply crops for several weeks after the rainy period. In many of these areas, a significant quantity of water is stored in seasonal shallow alluvial aquifers, located under dry riverbeds and in the vadose zone surrounding the small reservoirs. Except in the case of high altitude swamps, the availability of these areas determines the settlements of the population, the agricultural production of villages, and the price of properties in this semi-arid region. In these areas, small-scale agricultural schemes are predominant (Sampaio and Salcedo, 1997).

In some of these areas, thousands of small reservoirs were built to store water during the rainy season. After the rainy season, the water levels in the small reservoirs decline because of evaporation, and because of multiple domestic usage of water. In the dry season, recession agriculture is practiced on the borders of the reservoirs. In other words, recession agriculture consists of cropping the margins of reservoirs, on slight slopes, while the water level in the reservoirs progressively drops. In recession cultivation, the crop completes its growth cycle in the dry season, without consuming the total amount of water available. Recession cultivation is a very popular traditional technique, as it is the cheapest way to carry out irrigated agriculture without the cost of pumping. The cultivation is performed with different regional characteristics. The most primitive form of recession cultivation is not only to crop forage grass, but sweet potato, and other subsistence crops also are often grown. More evolved forms of recession cultivation feature more productive forage plants and cash crops, such as corn, bean and watermelon (Antonino and Audry, 2001). This possibility of cultivation during the dry season is essential for the livelihood of most of the small farmers who can rely on water availability for a given time interval. This contrasts with rainfed cultivation, which is far more subject to rainfall uncertainty.

Molle and Cadier (1992) published the only work related to recession cultivation in North-eastern Brazil, which discussed several procedures for water storage and use in small reservoirs, such as the selection of crops, and management issues. Molle (1991) estimated that in the Northeast of Brazil there are more than 70,000 small reservoirs. Similar cropping systems exist, especially in the flood plains of rivers in West Africa (in Senegal, Niger, etc.). However, very little work has been done on water dynamics in soils under recession cultivation conditions. This is partly explained by the complexity of the reservoir border conditions, where the soil surface evolves gradually from ponded to evaporating conditions as water regresses (Antonino et al., 2004).

This paper is focused on an analysis of the water in the reservoir border area. By a combination of modelling and monitoring the components of the water balance are determined for a period of 67 days.

2. The components of the integral water balance

The dynamics of the water in the system is analysed on the basis of the integral water balance of the soil profile in the form for a given time interval Δt (Fig. 1):

$$\Delta S = R - \mathrm{ET} - F \tag{1}$$

where ΔS is the change in soil water storage during time interval Δt; R the quantity of water infiltrating at the soil surface; ET the actual evapotranspiration, in the case of the bare soil ET becomes E the actual evaporation; F is the vertical water flux at the bottom of the profile. Eq. (1) applies to a volume of soil associated with a unit area of land to a certain depth, which implies that it is assumed that for this volume there is no net lateral inflow or outflow of water.

Field and laboratory experimentation is designed to evaluate the various terms in Eq. (1). The profile water storage S is determined by spatial integration of the profile of the volumetric water content θ measured with a neutron probe. The input R at the soil surface is determined by a rain gauge. The actual evapotranspiration ET is obtained from

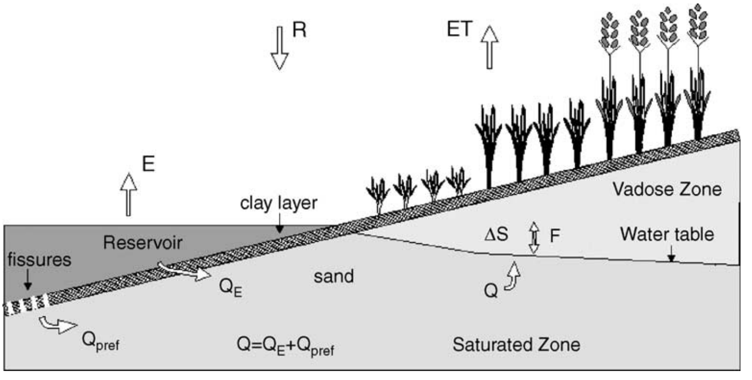

Fig. 1. Sketch of the water dynamics of a small reservoir–recession system, the reservoir, the unsaturated zone (vadose zone) and the phreatic aquifer (saturated zone) and associated fluxes (arrows): R is the rainfall, E and ET being respectively evaporation and evapotranspiration fluxes, F is the vertical water flux at the bottom of the soil profile, and Q is the total flux from the reservoir towards the aquifer which is composed of two terms: Q_{pref} preferential flow and Q_{E} the flow through the medium and ΔS is the change in soil water storage during Δt.

Eq. (1). The water flux F at the bottom of the profile is determined on the basis of Darcy's law:

$$F = -k\frac{\partial H}{\partial z} = -k\frac{\partial (h+z)}{\partial z} \quad (2)$$

where the total head H is the sum of the pressure head h and the gravitational z, and k is the hydraulic conductivity.

The use of Eq. (2) requires measurements of the gradient of pressure head h, the water content θ, and the hydraulic conductivity k at the bottom of the profile. The pressure head is measured with tensiometers, the water content with a neutron probe, and the hydraulic conductivity with a disk permeameter. To relate h, θ, and k, the van Genuchten–Mualem model (van Genuchten, 1980) is used:

$$\Theta(h) = \frac{\theta - \theta_r}{\theta_s - \theta_r} = [1 + |\alpha h|^n]^{-m}, \quad \text{with } m = 1 - 1/n \ (n > 1) \quad (3)$$

$$k(\theta) = k_s \Theta^{1/2}[1 - (1 - \Theta^{1/m})^m]^2 \quad (4)$$

where θ_s is the water content at saturation; θ_r the residual water content; α, m, and n the fitting parameters and k_s is the hydraulic conductivity at saturation.

The flux F can be calculated by Eq. (2), using the measured hydraulic gradients. However, as soil water content and pressure head were measured only once a day, an instantaneous capillary rise (F^i) was calculated, considering the geometric mean in depth of the hydraulic conductivity ($k(\theta)$) and the gradient of the total head ($\bigtriangledown H$), given by:

$$F^i = k(\theta)^i_{j+1/2} \nabla H^i_{j+1/2} \quad (5)$$

with

$$k^i_{j+1/2} = (k^i_j k^i_{j+1})^{1/2} \quad (6a)$$

$$\nabla H^i_{j+1/2} = \frac{H^i_j - H^i_{j+1}}{\Delta z_j} \quad (6b)$$

where the index j refers to depth of the layer, and the index i refers to time, representing the measurement day. This calculated instantaneous flux could not simply be integrated over the whole day, as it varies during the day according to the superficial evaporative demand.

The instantaneous evaporative demand over the day is usually considered as a sine function (Kirkham and Powers, 1972). Hence, it is assumed that the rate of capillary rise follows an equivalent pattern given by:

$$F^i = F_{max} \sin\left[2\pi\frac{(t - t_i)}{24}\right], \quad t_i \le t \le t_f \quad (7)$$

where F_{max} represents the maximum capillary rise flux, t the time of the day, t_i and t_f, respectively, the initial and final limits of the day time period during which capillary rise occurs. We chose to set these limits at 6 and 18 h (06:00 a.m. and 06:00 p.m.).

The cumulated capillary rise can be calculated from:

$$F = \int_6^{18} F^i \mathrm{d}t \quad (8)$$

Introducing Eq. (7) in Eq. (8) gives:

$$F = AF_{\max} \tag{9}$$

where A is a constant equal to 7.6394 for this specific time interval (6–18 h). A rational factor r between daily capillary rise (F), and instantaneous capillary rise rate (F^{i}) can be defined by:

$$r = \frac{F}{F^{\mathrm{i}}} = \frac{7.6394}{\sin\left[2\pi(t-6)/24\right]} \tag{10}$$

3. Material and methods

3.1. Study area and region

The study was performed in the recession zone of the basin of Flocos dam, municipality of Tuparetama, Pernambuco State (7°36′S and 37°18′W), in the semi-arid region in the Northeast of Brazil. The Flocos dam is more than 100 years old. The surface area that can be used for recession cultivation was estimated to be approximately 0.75 ha, and with a maximum water level in the reservoir of about 2.7 m above the lower part of the reservoir near the dam (Fig. 2).

The soil profile overlying the bedrock is uniform all over the reservoir. The soil, classified as Fluvent, consists of two distinct layers: a top clayey textured layer overlying sandy soil. The depth of the soil profile varies approximately between 2.1 m on the borders

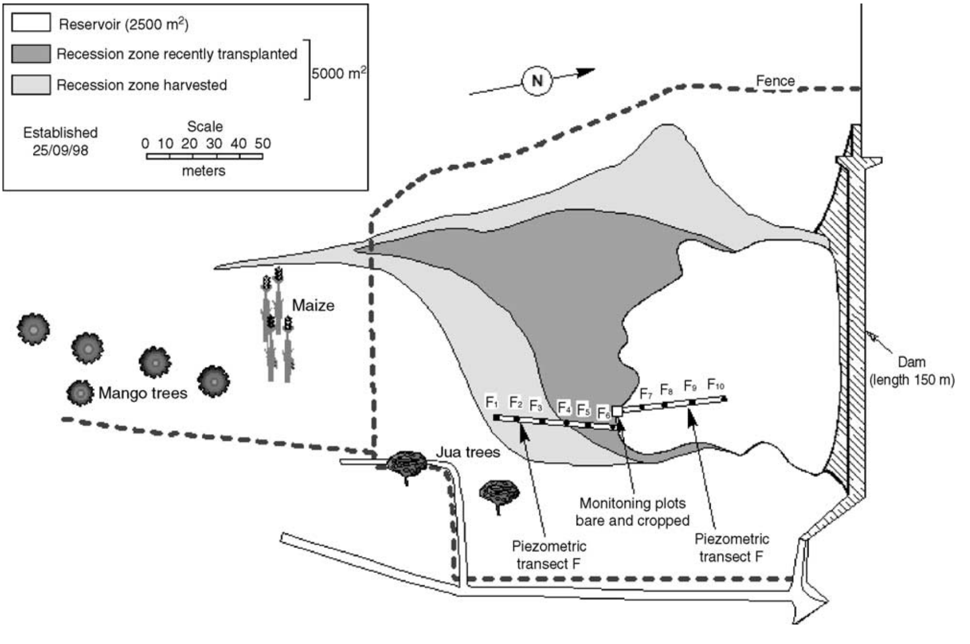

Fig. 2. Schematic map of the studied system, and location of the piezometers transects and experimental plots.

to 1.9 m in the deepest part of the reservoir. The soil thickness of the top clayey textured layer is 0.2 m for the whole reservoir, except for the deepest part of the reservoir, where it has a thickness of 0.5 m. During the dry season of 1998 the reservoir dried out completely and a network of fissures was observed at the bottom of the dam, which consisted of large fissures with an average width of 5 cm. The surface area of the reservoir where the network of fissures is located was estimated to be 600 m^2.

The water retention and hydraulic conductivity characteristics at the depth of 20, 40, 60, and 80 cm are presented in Section 3.3.

Rainfall in the semi-arid region is highly irregular, with precipitation concentrated in three to four consecutive months per year, between November and June. In the Tuparetama municipality region, the rainy season generally occurs in the period January–April.

3.2. Field plots monitoring program

Monitoring of the water dynamics in the reservoir/recession zone was performed during the period from October 1997 to December 1999. In the recession zone of the reservoir, two contiguous 3 m $\times$ 3 m plots were monitored, one with Marreca grass (*Paspalum conjugatum* Berg.) and the other one on bare soil. Marreca grass is a stoloniferous perennial graminoid, also called T grass or sour grass, and is often considered to be a weed in other parts of the world. Three weeks before the experiments, 25 cm high shoots that had been collected from the surrounding area, were transplanted at a density of 30 cm $\times$ 30 cm. The crop was harvested 2 months later at the flowering stage, after reaching a height of approximately 1 m. Close to the reservoir, a meteorological station was installed, equipped with automatic sensors: a rain gauge, a thermometer and an anemometer, for recording respectively rainfall, air temperature and wind speed, as well as a class "A" tank for measuring pan evaporation. In the reservoir, the water level was recorded with a set of limnimetric scales. In the plots, a 1-m access tube for neutron probe measurements, and a set of tensiometers for 10, 20, 30, 40, 60, and 80 cm depths were installed and monitored daily. The neutron probe (Humisol Solo 20, Nardeux Co., France) was calibrated for normalised counts (C/C_0, where C_0 is the number of counts in water) with gravimetric water content measurements. The calibration was performed at 30 points for the entire profile with volumetric water content values ranging from 0.05 to 0.45 and fitted to a linear regression: $\theta = (0.75164C/C_0) - 0.00185$ with a regression coefficient r^2 of 0.96408. A transect of 10 piezometers was installed to monitor the daily water table levels in the recession area (Fig. 2).

The measurements of the soil water potential were taken once a day in the morning, between 8:30 and 11:00, with 9:00 being the most frequent measurement time. Hence, it was found that the r values ranged from 12.6 to 7.6 as shown in Fig. 3. Actual evaporation E can then be calculated with Eq. (1).

Rainfall distribution during the period ranging from November 1997 to October 1999 is shown in Fig. 4a. Precipitation during the period December 1997 to May 1998 was higher than the precipitation during the whole of 1998. In December 1997, two rainfall events (11 and 25 December) represented 85.4% (171.1 mm) of the total monthly rainfall. In May 1999, two rainfall events (5 and 17 May) corresponded to 46.5% of the total monthly precipitation (Fig. 4b).

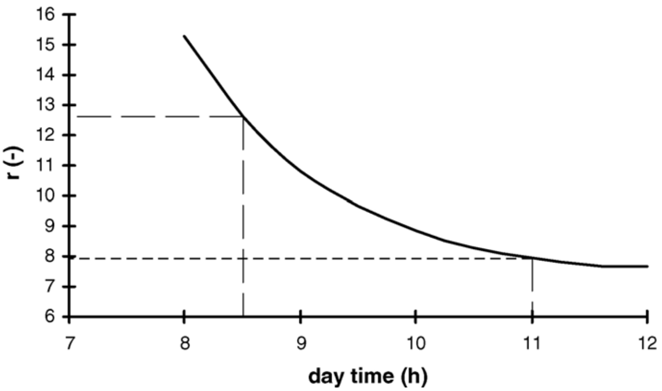

Fig. 3. Evolution of factor r during daytime for the time interval of the experimental measurements.

The annual pan evaporation, E_{pan}, for 1998 was 3592.7 mm. The minimum (in July) and maximum (in December) reference evaporation rates were 5.3 and 8.9 mm day^{-1}, respectively. The annual average air temperature is 26.1 °C, with minimum and maximum values of 16.5 and 34.8 °C, respectively.

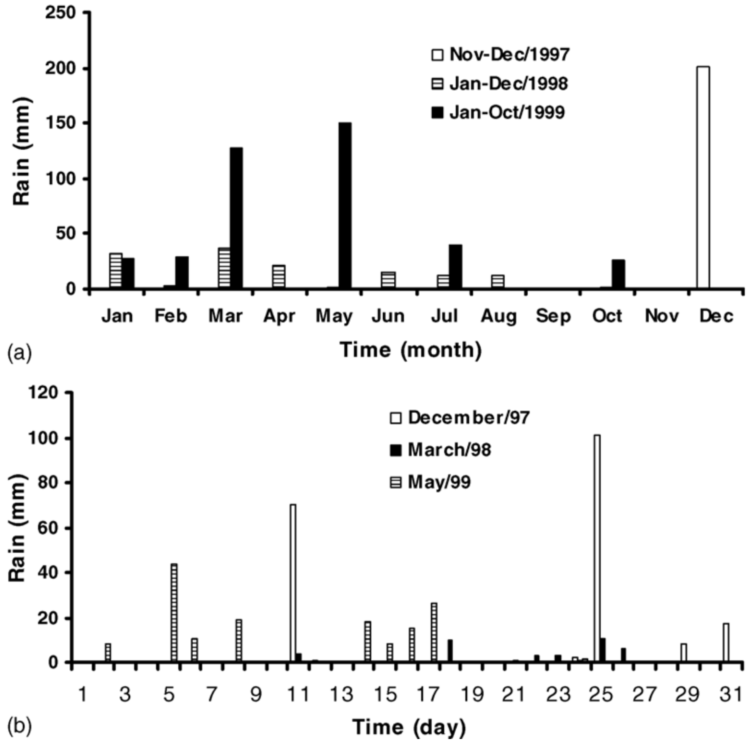

Fig. 4. Rainfall distribution in the study site: (a) November 1997 to October 1999 (monthly); (b) December 1997, March 1998 and May 1999 (daily).

The reference evapotranspiration ET_0 was estimated using the following relationship (Doorenbos and Pruitt, 1977):

$$ET_0 = K_p E_{pan} \tag{11}$$

where K_p is the pan coefficient, depending on the pan environment in relation to the nearby soil surface and climatic conditions (Rana and Katerji, 2000). Considering the guidelines provided by Doorenbos and Pruitt (1977), or Allen et al. (1998) with a moderate wind speed (2–5 m s^{-1}), a green fetch of 1 m, and medium values of relative humidity (of 40–70%), the coefficient was estimated to be 0.75, which is consistent with the average value of 0.7 determined in semi-arid conditions (Jensen et al., 1990). The annual reference evaporation for 1998 was found to be 2694 mm.

The water balance components were determined for 67 days, from 29 September to 5 December 1998. The water balance components in the bare soil plot were calculated for the 0–30 cm soil layer, while in cropped soil the water balance was calculated in the 0–100 cm layer, as it corresponded to the root zone for Marreca grass.

For the bare soil plot, hydraulic conductivity values were calculated for the depths $j = 20$ cm and $j + 1 = 40$ cm during the entire study period, while in cropped soil the considered depths were $j = 20$ cm and $j + 1 = 40$ cm from the 29 September to 19 October, $j = 40$ cm and $j + 1 = 60$ cm from 20 to 30 October, and $j = 60$ cm and $j + 1 = 80$ cm from the 31 October until the end of study period.

3.3. Soil characteristics

As pointed out in Section 3.1, at the location of the bare and cropped soil plots, the soil profile consists of a 20-cm top clayey textured layer overlaying a sandy soil. Table 1 shows dry bulk density and texture data to 120 cm in depth. The bulk density increases with depth along the profile from 1.42×10^3 to 1.66×10^3 kg m^{-3} (Table 1), inversely to clay content.

Table 2 shows the parameters of the van Genuchten–Mualem model for the water retention and hydraulic conductivity characteristics, as defined by Eqs. (3) and (4). The parameters for the water retention curves were obtained by fitting Eq. (3) to experimental field and laboratory data (Fig. 5). In order to simplify the fitting procedure θ_r was set to 0 according to the method described by Wessolek et al. (1994). During the monitoring period, simultaneous measurements were taken of the pressure head h with tensiometers

Table 1
Texture and dry bulk density (ρ) of the soil

Depth (cm)	ρ^a ($\times 10^3$ kg m^{-3})	Sand	Silt (%)	Clay
5–15	1.43 ± 0.03	30.3	25.6	44.1
15–25	1.42 ± 0.01	38.0	20.7	41.3
25–35	1.53 ± 0.02	76.2	8.4	15.4
35–45	1.58 ± 0.05	85.2	5.7	9.1
50–70	1.58 ± 0.02	90.2	2.5	7.3
70–90	1.63 ± 0.03	85.9	4.6	9.5
90–110	1.66 ± 0.01	88.1	3.4	8.5

[a] Mean and standard deviation from three samples.

Table 2
Parameters of the van Genuchten–Mualem model (Eqs. (3) and (4)), including the hydraulic conductivity at saturation, for four depths

Depth (cm)	θ_r (cm^{-3} cm^{-3})	θ_s (cm^{-3} cm^{-3})	α[a] (cm^{-1})	n[a]	k_s[b] ($cm\ h^{-1}$)
20	0.0	0.466	0.0041 ± 0.00218	1.1176 ± 0.04326	0.59 ± 0.05
40	0.0	0.387	0.0283 ± 0.00315	1.2125 ± 0.01130	2.56 ± 0.45
60	0.0	0.352	0.0792 ± 0.0163	1.1785 ± 0.01394	54.56 ± 14.73
80	0.0	0.338	0.0252 ± 0.00228	1.306 ± 0.01616	11.81 ± 14.73

[a] Fitted values and standard deviation.
[b] Mean and standard deviation.

and the water content θ with the neutron probe. The data were complemented by laboratory water retention data, obtained with a pressure plate apparatus (Reeve and Carter, 1991).

Hydraulic conductivity near saturation was only determined in situ, using a disk permeameter (Angulo-Jaramillo et al., 2000) with the Zhang (1997) method. The soil hydraulic properties are assumed to be uniform and representative for both plots. The hydraulic conductivity at saturation is constant in the top 0–40 cm layer, whereas it increases drastically at 60 cm, and then reduces at 80 cm (Fig. 6).

4. Results and discussion

4.1. Integral water balances of the bare and cropped soil plots

Fig. 7 shows the evolution, from 29 September to 5 December 1998, of the water content profiles in the bare and cropped soil plots. Higher water content variations were

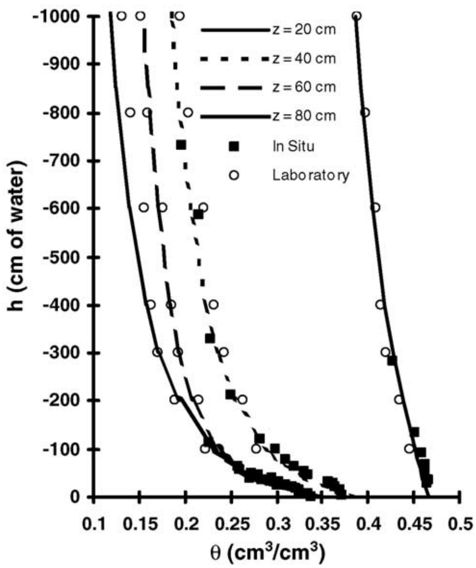

Fig. 5. Soil–water retention curves obtained in situ and in the laboratory, and fitted to the van Genuchten model.

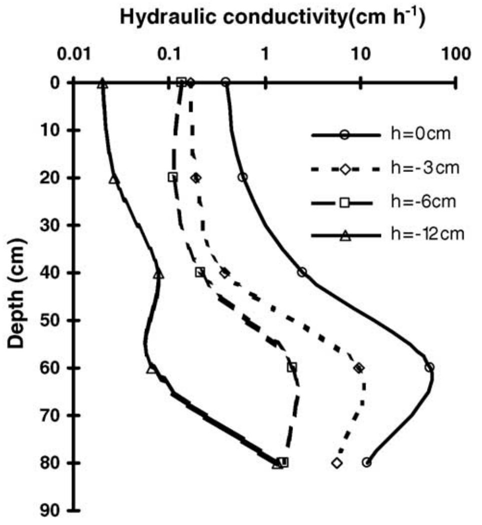

Fig. 6. Hydraulic conductivity profiles obtained from four different potentials using a disk permeameter.

recorded in the cropped plot than in the bare soil plot, as a result of the water uptake by the root system.

In order to highlight the calculation procedures an example is presented here. For the bare soil plot, at 9:00 on 13 October the water content and the total head for 20 and 40 cm depths were 0.463 and 0.364, and −86.6 and −60.2 cm, respectively. Hence, the hydraulic

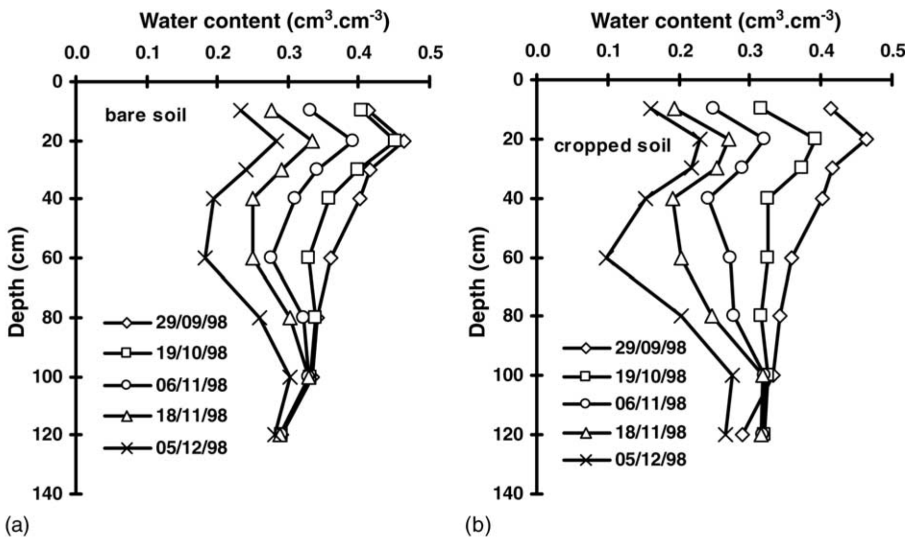

Fig. 7. Soil water content profiles at different dates for the (a) bare and (b) cropped soil plots.

Table 3
Components of the water balance for bare and cropped soils from 29 September to 5 December 1998

	ΔS (mm)	F (mm)	ET (mm)	ET_d (mm day^{-1})
Bare soil				
29 September–10 October	−1.5	80.3	81.8	7.4
11 October–19 October	−1.7	73.2	74.9	8.3
20 October–30 October	−11.2	76.1	87.3	7.9
31 October–10 November	−12.0	55.4	67.4	6.1
11 November–21 November	−16.6	16.2	32.8	3.0
22 November–29 November	−7.2	2.1	9.3	1.3
30 November–5 December	−3.6	1.1	4.7	0.7
Cropped soil				
29 September–10 October	−11.2	101.4	112.6	10.2
11 October–19 October	−26.2	75.9	102.2	11.4
20 October–30 October	−32.8	80.5	113.2	10.3
31 October–10 November	−38.7	68.0	106.7	9.7
11 November–21 November	−49.5	28.0	77.5	7.0
22 November–29 November	−24.9	3.0	27.9	4.0
30 November–5 December	−20.1	2.1	22.3	3.2

ΔS, change in soil water storage; F, capillary rise; ET, actual evapotranspiration; ET_d, daily actual evapotranspiration.

conductivity values calculated with Eq. (4) were respectively 0.412 and 0.862 mm h^{-1} with a geometric mean computed with Eq. (6a) of 0.596 mm h^{-1}.The hydraulic gradient calculated with Eq. (6b) being 1.3. The instantaneous capillary rise (F^i) given by Eq. (5) was 0.79 mm h^{-1}, the factor r of Eq. (10) was 10.8 and finally the daily capillary rise (F) was 8.51 mm.

Table 3 shows the components of the water balance for various periods. During the monitoring period, no precipitation was recorded, the hydraulic gradients in the soil profiles show that during the entire monitoring period the water flow at the bottom was directed upwards. Fig. 8 shows that during the monitoring period, the water table level decreased by 100 cm, at the same constant rate for both experiments.

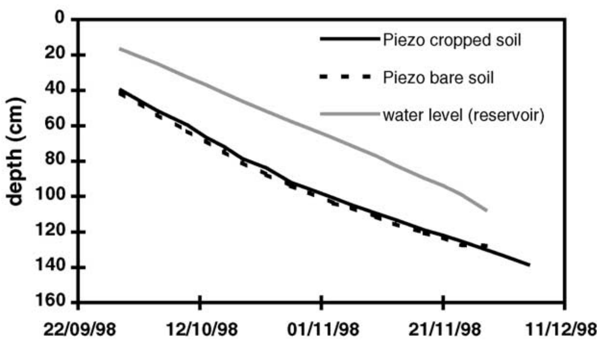

Fig. 8. Evolution of water table depth and the water level in the lake, taking the soil level near the piezometers as reference, during the monitoring period.

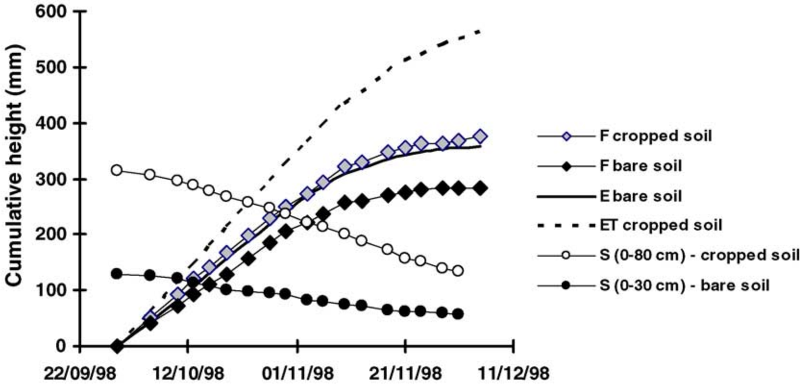

Fig. 9. Evolution of the components of the water balance under bare and cropped conditions. *F*, capillary rise; *E*, actual evaporation; ET, actual evapotranspiration; *S*, soil water storage.

For the bare and cropped soils, respectively, the cumulative actual evaporation values (Fig. 9) calculated with Eq. (1) were 358.3 and 562.4 mm, the cumulative capillary rise computed with Eqs. (5)–(10) were 304.4 and 358.9 mm, and the soil water storage variations were 53.8 and 203.4 mm. The average values for actual evaporation and evapotranspiration rate were 5.3 and 8.4 mm day^{-1}, respectively, and the average value for reference evaporation rate ET_0 was 8.7 mm day^{-1}.

Fig. 10 shows the variations in time of the ratio between actual evaporation/evapotranspiration (ET) and reference evapotranspiration (ET_0) for the bare and cropped soil plots. These curves present very similar shapes, attesting to a similar hydrological behaviour during the drying out period. During the first 42 days after the beginning of the monitoring period, the actual evapotranspiration on cropped soil was at its maximum value, and an average value of 1.2 for the ratio ET/ET_0 was found.

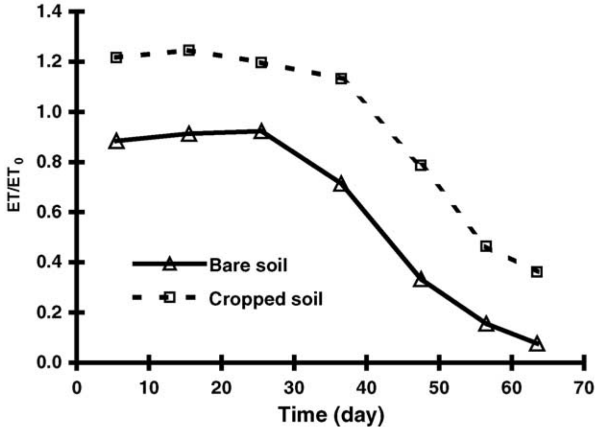

Fig. 10. Ratio between actual evapotranspiration (ET) and reference evapotranspiration (ET_0) in the bare and cropped soil plots.

This ratio ET/ET_0, denominated crop coefficient K_c, represents an integration of the effects that distinguish the crop ET from the reference ET_0 (Rana and Katerji, 2000). Generally, the K_c curve reflects an initial stage with low values and then a rising limb during increased growth and a peak where the crop attains maximum cover and growth followed by a decreasing limb when leaves start shedding at the end of the growth cycle (Abdelhadi et al., 2000).

The initial values obtained for K_c were high and differed from the low values usually reported in literature. This can be partly explained by the fact that 25 cm high shoots of Marreca grass (*Paspalum conjugatum* Berg.) had already been transplanted 3 weeks before the monitoring started while the area was still submersed. Therefore, the crops were already in full ground cover condition (mid-season stage), when the experiment started the cropping factor had probably almost reached its maximum value. In the bare soil plot during the first drying out stage, an average ratio value of the E/ET_0 of 0.9 was found (Fig. 8).

4.2. Soil water dynamics in the bare and cropped soil plots

As described by Idso et al. (1974), and shown by the data in Fig. 10 and Table 3, during the drying out process of the upper soil layers under natural conditions, without vegetation, three characteristic stages may be distinguished. In the first stage, when the soil water content is high, the evaporation rate is controlled by the climatic conditions, and the actual evaporation rate corresponds to the potential rate. During the second stage, when the soil water storage starts to decline, the evaporation process is controlled by the soil conditions related to its ability to conduct water from the lower to the upper layers. In the third stage, the soil is completely dry near the soil surface, and the hydraulic continuity along the profile towards the surface no longer exists, and the evaporation process is controlled by the vapour transfer mechanisms and by adsorption in the soil matrix.

The results obtained from the monitoring program show the difference in the soil water dynamics for the bare and cropped soil plots, related to the stages previously described. Table 3 shows that in the first stage, corresponding to the first 31 days after the beginning of the experiment, the soil water storage of the bare soil decreased by 14.4 mm, while for the cropped soil the amount of water storage decreased by 70.2 mm. In the case of the bare soil, the water transfer dynamics during this stage was initially characteristic of steady state flow conditions, with an extremely small variation in soil water storage. Actual evaporation was equal to the atmospheric evaporative demand, with maximum evaporation rate close to capillary rise flux from the water table. For the cropped soil, the large decrease in soil water storage was due to the water uptake from the roots close to the soil surface.

During the second stage, corresponding to the following 29 days, the soil water storage decreased by 35.6 mm in the bare soil plot, whereas in the cropped soil plot the soil water storage decreased by 113.1 mm. The water storage in the vadose zone increasingly contributed to evaporation, whereas the contribution from capillary rise decreased progressively as the water table fell.

During the last 7 days of the third stage, the soil water storage decreased by 3.6 and 20.1 mm, in the bare and cropped soil plots, respectively. The variation in the soil water

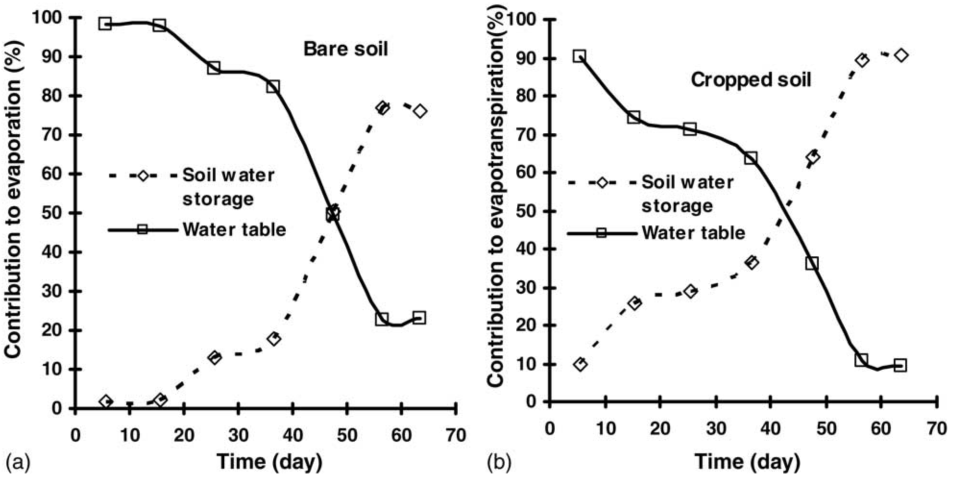

Fig. 11. Evaporation and evapotranspiration contribution (%) from the water storage in the vadose zone and from the water table, in the bare (a) and cropped (b) soil plots, respectively.

storage in the upper layers was very low or even null, the contribution from the water table was negligible, and evaporation was very low.

During the first stage, the average contribution from capillary rise in the bare soil plot was 94% (Fig. 11a), whereas in the cropped soil plot, it was 78% (Fig. 11b). During the second stage the contribution from capillary rise was about 51% for the bare soil plot and about 37% for the cropped soil plot. Finally, the average contribution from capillary rise was 23% for the bare soil plot, and 10% for the cropped soil plot during the third stage (Fig. 10a and b).

During the three successive stages, the water table level drawdown was 39.3, 51.5, and 8.5 cm, respectively, representing a total of 1 m. Considering equilibrium profiles for pressure head above the water table, the corresponding water content and water storage was computed from retention curve parameters (Table 2), for the initial and final situation. The water storage was found to be 354 and 297 mm at the beginning and the end of the monitoring period, respectively. On the other hand, following a similar procedure as described by De Voos et al. (2000, 2002), the vertical flux at the bottom of the profile, namely capillary rise F, can be roughly estimated as being the sum of the water table drawdown Q_{TD} and the lateral recharge of the aquifer Q_{TR} and Eq. (1) becomes:

$$\Delta S = (Q_{TD} + Q_{TR}) - \mathrm{ET} \tag{12}$$

Over the entire monitoring period, the cumulative contribution of the water table drawdown (Q_{TD}) was found to be 57.2 mm, whereas the cumulative soil evaporation and evapotranspiration were 358 and 562 mm for the bare and cropped soil, respectively. At the same time ΔS in bare and cropped situations was -55.6 and -203.4 mm, respectively. According to Eq. (12), the contributions of aquifer recharge to evaporative demand are 245 mm for bare soil and 301 mm for cropped soil, which represents 68 and 54% of the total evaporation and evapotranspiration, respectively. During the first stage, when hydraulic continuity existed between the water table and soil surface in the vadose zone, the contribution of the reservoir towards the water table was 208 and 236 mm, while the cumulative evaporation and evapotranspiration were 244 and 328 mm for the bare and cropped soils, respectively. Hence, the aquifer recharge, mainly from the reservoir, represented 85 and 72% of the cumulative evaporation and evapotranspiration. These results clearly prove that the transmission between the reservoir and the aquifer was very efficient.

4.3. Water transfer in the system reservoir–recession

As shown in Fig. 8, the piezometric level is always lower than the water level in the reservoir, implying a continuous hydraulic gradient from the reservoir towards the water table. This indicates that the reservoir recharges the aquifer underneath the recession zone.

A network of fissures in the deepest part of the reservoir affects the clayey layer through its entire thickness, and connects the underlying sandy layer directly with the reservoir water. The presence of these fissures was witnessed when the reservoir was completely dried out. However, since this material is not constituted of swelling 2:1 clay minerals, the fissures remain open after new submersion. Consequently, this network of fissures at the bottom of the reservoir contributes efficiently to the recharging of the aquifer underneath the recession zone, and offers possibilities for cropping activities in this area.

5. Concluding remarks

In the Northeast of Brazil, small reservoirs are typically used for small-scale irrigated agriculture, especially for recession cultivation on the border of the reservoirs during the dry season. During this period, the crop is supplied with water by capillary rise from the phreatic aquifer, which is connected to the small reservoir. Consequently, the knowledge of water dynamics in small reservoir–aquifer systems is crucial for the purpose of planning and management, including crop selection and irrigated surface area, based on water requirements, duration of growth cycle, tolerance to water stress and/or excess in the root zone.

A monitoring program was established in a typical system of the Northeast of Brazil under semi-arid conditions, and used for the development of small-scale irrigation. Based on the data from this monitoring program, the water balance was calculated, on a plot scale and in the presence of water table, for two different conditions: bare soil and cropped soil. The calculation of the terms of the water balance allowed the identification of different stages in terms of soil water dynamics, conditioning evaporation, evapotranspiration, capillary rise and water table drawdown in the phreatic aquifer.

The water balance was calculated, for both the cropped and the bare soil plots, during a period of 67 days (29 September to 5 December 1998) without precipitation. The annual reference evapotranspiration for 1998 was 2694.5 mm, and the total precipitation for the year was 153 mm. In the bare soil plot, the water balance was determined for the top 30 cm soil layer. During the monitoring period, the actual evaporation was 351.5 mm, the capillary rise was 304.4 mm, and the water storage variation in the 0–30 cm layer was

53.8 mm. The average value for the actual evaporation rate was 5.0 mm day^{-1}. In the cropped soil plot, during the monitoring period the actual evaporation was 562.4 mm, the capillary rise was 358.9 mm, and the variation in soil water storage in the 0–100 cm layer was 203.4 mm. The average value for the actual evapotranspiration rate was 8.4 mm day^{-1}, the average reference evapotranspiration being 8.7 mm day^{-1}.

This system, which is representative of a regional situation, is very old and its flow conditions are affected by the accumulation of a thick sedimentary layer of fine particles, therefore, being potentially impermeable. However, field observation and water balance suggested the occurrence of preferential flow due to the presence of fissures in the bottom of the small reservoir. This preferential flow is beneficial for the maintenance of an adequate flow of water towards the land along the borders of the reservoirs and helps in the use of this kind of system. The study of water dynamics in small reservoir–recession systems is fundamental for the sustainable development of agriculture, in terms of water conservation, at the same time as maximum crop yield is achieved.

Acknowledgements

We thank the CNPq (National Research Council, Brazil), the IRD (Research Institute for Development, France) and the cooperation project CAPES-COFECUB (no. 350/01) for providing financial support to this study.

References

Abdelhadi, A.W., Hata, T., Tanakamaru, H., Tada, A., Tariq, M.A., 2000. Estimation of crop water requirements in arid region using Penman-Monteith equation with derived crop coefficients: a case study on Acala cotton in Sudan Gezira irrigated scheme. Agric. Water Manage. 45, 203–214.

Allen, R.G., Pereira, L.S., Raes, D., Smith, M., 1998. Crop Evapotranspiration: Guidelines for Computing Crop Water Requirements. Irrigation and Drainage, Paper No. 56, FAO-ONU, Rome, 300 pp.

Angulo-Jaramillo, R., Vandervaere, J.P., Roulier, S., Thony, J.-L., Gaudet, J.P., Vauclin, M., 2000. Field measurement of soil surface hydraulic properties by disc and ring infiltrometers. A review and recent developments. Soil Till. Res. 55, 1–29.

Antonino, A.C.D., Audry, P. (Eds.), 2001. Utilização de Água no Cultivo de Vazante no Semi-Árido do Nordeste do Brasil. Recife: Editora Universitária UFPE-IRD (in Portuguese).

Antonino, A.C.D., Angulo-Jaramillo, R., Hammecker, C., Netto, A.M., Montenegro, S.M.L.G., Lira, C.A.B.O., Cabral, J.J.S.P., 2004. A simplified water transfer model of the reservoir–recession system, including preferential flow, in semi-arid region in North-eastern Brazil. J. Hydrol. 287, 147–160.

Doorenbos, J., Pruitt, W.O., 1977. Guidelines for Predicting Crop Water Requirements. Irrigation and Drainage, Paper No. 24 (Review), FAO-ONU, Rome, 144 pp.

De Voos, J.A., Hesterberg, D., Raats, P.A.C., 2000. Nitrate leaching in a tile drained silt loam soil. Soil Sci. Soc. Am. J. 64, 517–527.

De Voos, J.A., Raats, P.A.C., Feddes, R.A., 2002. Chloride transport in a recently reclaimed Dutch polder. J. Hydrol. 257, 59–77.

Idso, S.B., Reginato, R.J., Kimball, B.A., Nakayama, F.S., 1974. The three stages of drying of field soil. Soil Sci. Soc. Am. Proc. 38, 831–835.

Jensen, M.E., Burman, R.D., Allen, R.G. (Eds.), 1990. Evapotranspiration and Irrigation Water Requirements. ASCE Manuals and Reports on Engineering Practice No. 70. American Society of Civil Engineers, New York.

Kirkham, D., Powers, W.L., 1972. Advanced Soil Physics. Wiley Interscience, New York.
Molle, F. 1991. Carctéristiques et potentialités des açudes du nordeste brésilien. Thèse de doctorat. Univeristé de Montpellier (in French).
Molle, F., Cadier, E. (Eds.), 1992. Manual do Pequeno Açude. SUDENE-ORSTOM, Recife (in Portuguese).
Rana, G., Katerji, N., 2000. Measurement and estimation of actual evapotranspiration in the field under Mediterranean climate: a review. Agric. For. Meteorol. 13, 125–153.
Reeve, M.J., Carter, A.D., 1991. Water release characteristic. In: Smith, K.A., Mullins, C.E. (Eds.), Soil Analysis—Physical Methods. Marcel Dekker, Inc., New York, (Chapter 3), pp. 111–160.
Sampaio, E.V.S.B., Salcedo, I.H., 1997. Mesa Redonda para o manejo sustentável dos solos brasileiros. XXVI Congresso Brasileiro de Ciência do Solo, Rio de Janeiro, 1997, CD-ROM (in Portuguese).
van Genuchten, M.T., 1980. A closed-form equation for predicting the hydraulic conductivity of unsaturated soils. Soil Sci. Soc. Am. J. 44, 892–898.
Wessolek, G., Plagge, R., Leij, F.J., van Genuchten, M.T., 1994. Analysing problems in describing field and laboratory measured soil hydraulic properties. Geoderma 64, 93–110.
Zhang, R., 1997. Infiltration models for the disc infiltrometer. Soil Sci. Soc. Am. J. 61, 1597–1603.